

Goose astrovirus infection affects uric acid production and excretion in goslings

Wankun Wu,^a Rong Xu,^a Yingjun Lv,¹ and Endong Bao

MOE Joint International Research Laboratory of Animal Health and Food Safety, College of Veterinary Medicine, Nanjing Agricultural University, Nanjing 210095, China

ABSTRACT In 2018, a new goose astrovirus (GAstrV) was reported in China, which causes 2 to 20% deaths in 4- to 16-day-old goslings causing great damages to the livestock industry. Gout is the typical feature of GAstrV infection in goslings. However, the mechanism of gout formation remains unclear. In the present study, 2-day-old goslings were infected intramuscularly with GAstrV for 14 D. One quarter of the infected goslings died, and typical gout pathological changes were found in the dead infected goslings. Pathological changes were observed in the morphology of the kidney and liver, such as degeneration, necrosis, and inflammatory cell infiltration. Accordingly, a high virus load was found in both organs. The serum level of uric acid in the inoculated goslings was higher, whereas

no differences were found in levels of creatinine, calcium, and phosphorus. Moreover, the xanthine dehydrogenase (XOD) and adenosine deaminase (ADA) activities and the mRNA levels of xanthine dehydrogenase, adenosine deaminase, phosphoribosyl pyrophosphate amidotransferase, and phosphoribosyl pyrophosphate synthetase 1 in livers increased, whereas the multidrug resistance-associated protein 4 mRNA level and Na-K-ATPase activity in the kidneys decreased. These results showed that GAstrV infection could cause lesions on the liver and kidney and then increase the expression or activity of enzymes related to uric acid production in the liver and decrease renal excretion function, which contribute to hyperuricemia and gout formation.

Key words: goose astrovirus, gosling, gout, hyperuricemia, uric acid

2020 Poultry Science 99:1967–1974

<https://doi.org/10.1016/j.psj.2019.11.064>

INTRODUCTION

Astroviruses are small, non-enveloped, single-stranded, and positive sensed RNA viruses typically <35 nm in diameter. The polyadenylated genome of these viruses in size range from 6.2 kb (human) to 7.7 kb (duck) and consists of a 5'-untranslated region followed by 3 open reading frames (ORF), a 3'-untranslated region and a poly-A tail (Cortez et al., 2017). Based on their ability to infect avian and mammalian species, astroviruses are divided into 2 main genera, mamastrovirus and avastrovirus. Avastrovirus mainly infects turkeys, chickens, and ducks and can cause different diseases in the different host, including growth retardation, enteritis, kidney disease, visceral gout, hatchability problems, “white chick” in chickens (Smyth, 2017), and hepatitis in ducklings (Sandhu et al., 1992; Todd et al., 2009). Until 2018, there were no

reports of goose infection with astroviruses. Recently, several studies reported a new goose astrovirus (GAstrV), which causes gosling visceral gout and results in 2 to 20% death in 4- to 16-day-old gosling in China. This virus was genetically distinct from known astroviruses, forming a distinct clade according to the amino acid sequence of the full-length ORF2 protein (Zhang et al., 2018a, 2018b; Jin et al., 2018; Niu et al., 2018; Yang et al., 2018; Yuan et al., 2019). This new goose astrovirus is a newly emerging pathogen that causes great damage to the goose industry; therefore, more attention should be paid to reducing the damage caused by this virus to goslings. Visceral gout is the typical characteristic in gosling infected with GAstrV. However, the mechanism by which gout is induced by GAstrV is unclear.

Gout is caused by the nucleation and growth of monosodium urate crystals in tissues in and around the joints, following long-standing hyperuricemia. Hyperuricemia occurs as a result of overproduction of uric acid from hepatic metabolism or renal underexcretion (Dalbeth et al., 2016). The liver is the mainly site of uric acid production, which occurs via purine metabolism of exogenous food sources and endogenous byproducts of cellular metabolism, using a series of enzymes such as xanthine

© 2020 The Authors. Published by Elsevier Inc. on behalf of Poultry Science Association Inc. This is an open access article under the CC BY-NC-ND license (<http://creativecommons.org/licenses/by-nc-nd/4.0/>).

Received August 3, 2019.

Accepted November 27, 2019.

^aThese authors contributed equally to this work.

¹Corresponding author: lyj@njau.edu.cn

oxidoreductase and adenosine deaminase (ADA). Renal excretion accounts for around two-thirds of urate excretion in mammals (Mandal and Mount, 2015), and this process is controlled by a suite of apically and basolaterally expressed secretory and reabsorptive molecules, such as urate transporter 1, organic anion transporter 1 (OAT1), OAT2, OAT4, and multidrug resistance-associated protein 4 (MRP4) (Nigam and Bhatnagar, 2018). Unlike in great apes, no significant facilitated reabsorption of urate was detected in chicken renal proximal tubules (Gutman and Yu, 1972; Brokl et al., 1994; Dudas et al., 2005). The ATP-driven secretory efflux pump, MRP4, and OAT were considered as important transport proteins in urinary secretion in avian systems (Hasegawa et al., 2007; Bataille et al., 2008).

Based on above information that GAstrV infection induced serious gout in goslings and that the liver and kidney are responsible for uric acid production and secretion, respectively, we hypothesized that GAstrV infection causes changes to enzymes related to purine metabolism and secretory molecules. Hence, in the present study, 2-day-old goslings were infected with GAstrV to establish a gout model, and then the parameters associated with uric acid production in the liver and transport proteins in kidney were investigated.

MATERIAL AND METHODS

Virus

The GAstrV-JSHA isolate (GenBank accession no. MK125058) was isolated from diseased goslings with gout in Jiangsu province, China, following serial passage in goose embryos and kept in our laboratory. The titer of the GAstrV-JSHA was $1 \times 10^{4.25}$ 50% tissue culture infective dose (TCID₅₀)/ml as determined by titration on goose kidney epithelial cells according to the method of Reed & Muench.

Animal Experiment

Before animal experiment, 5 1-day-old goslings were euthanized with intravenous pentobarbital sodium. No gross changes were found in all organs, and no GAstrV RNA was detected from kidneys and livers using RT-PCR method. Then 20 two-day-old goslings were placed in an animal isolator that were ventilated under negative pressure without any immunizations. These goslings were challenged with 0.5 mL GAstrV by intramuscular inoculation. Another 20 goslings were inoculated with 0.5 mL of phosphate buffered saline which served as negative control group. All geese were monitored daily for the occurrence of clinical signs for 14 D. During the experiment, both infected and uninfected geese were weighed, and blood samples from the wing vein were collected at 7 and 14 d postinfection (dpi). At 14 dpi, all the surviving goslings were euthanized with intravenous pentobarbital sodium. The gross changes of heart, liver, spleen, lung, kidney, intestine, pancreas, and brain were examined and collected. A portion of these tissues

were fixed in 10% formaldehyde for histopathological examination. The rest were stored at -80°C for further experiments. All animal procedures were approved by the Institutional Animal Care and Use Committee of Nanjing Agricultural University.

Histopathological Examination

The tissue samples were fixed in 10% formaldehyde and dehydrated by a series of alcohols, clarified in xylene, and embedded in paraffin. Then samples were sliced serially into 4 μm sections and stained with hematoxylin and eosin by routine methods. Stained sections were examined with a light microscope.

Serum Uric Acid, Creatinine, Calcium, and Phosphorus Detection

Blood samples were collected and centrifuged at 3,000 rpm to obtain serum. Levels of uric acid, creatinine, calcium and phosphorus in the serum were measured using commercial kits (Beyotime Institute of Biotechnology, Haimen, China) according to the manufacturer's protocols.

Detection of xanthine dehydrogenase, ADA, and Na-K-ATP Activities

Tissue weighing 0.1 g taken out from liquid nitrogen was placed in 1 mL cold physiological saline and grounded with a tissue pulping machine at 12,000 rpm in an ice-water bath. The tissue homogenate was centrifuged for 10 min at 4°C and 3,000 rpm by Sorvall Biofuge Strator centrifuge. The sediment was discarded, and the supernatant was 10% tissue homogenate. The total protein concentrations of this homogenate was detected with BCA protein assay kit (Thermo, Rockford, IL). The activity of ADA, xanthine dehydrogenase (XOD), and Na-K-ATP was measured by commercial kits (Beyotime) according to the manufacturer's protocols.

Detection of Transcripts of the ADA, XOD, Phosphoribosyl pyrophosphate amidotransferase, phosphoribosyl pyrophosphate synthetase 1, and MRP4 Genes by Real-Time PCR

Total RNA was extracted using Trizol (Invitrogen, Carlsbad, CA), and reverse transcription of the RNA was conducted using the HiScript Q RT SuperMix Kit (Vazyme, China). A Thermocycler (AB7300; Life Technologies, Carlsbad, CA) was used for quantitative PCR. Primer 5.0 software was used for the designation of the related genes including ADA, XOD, phosphoribosyl pyrophosphate amidotransferase (PRPPAT), phosphoribosyl pyrophosphate synthetase 1 (PRPS1), and MRP4 (Table 1). RNA expression was normalized by quantification of GAPDH as a housekeeping gene. Each sample was prepared in 3 duplicate tubes. Specific

gene expression was quantified using the $2^{-\Delta\Delta CT}$ method.

Statistical Analysis

The differences between the control group and experimental group were analyzed by Student *t* test. The results are expressed as the mean \pm standard deviation. $P < 0.05$ was considered to indicate a statistical significance compared with the control group, and $P < 0.01$ was considered to indicate a high degree of significance compared with the control group.

RESULTS

Clinical Examination

Twenty 2-day goslings were injected intramuscularly with 0.5 mL of GAstrV. No death or obvious clinical signs were observed in the noninoculated control. However, a reduction in body weight was noted from 12 dpi to the end of the experiment in the GAstrV-infected birds. The average body weight in the infected group at 12 and 14 dpi was significantly lower than that of control (12 dpi, 405.9 ± 77.1 vs. 491.5 ± 64.7 ; 14 dpi, 593.7 ± 85.6 vs. 686.9 ± 56.6) ($P < 0.05$). Moreover, 5 of the 20 infected goslings died during the experiment. At autopsy, the organs in the control group were normal (Figure 1A–D), whereas pathological changes typical of gout were found in the dead infected goslings, such as urate disposition on the surface of the liver, heart, and kidney, and in bile sacs and articular cavity and swelling and pale kidneys with white urate in the ureters (Figure 1E–H). In addition, no gout-related pathological changes, only swelling and pale kidneys, were found in most surviving infected goslings.

Histopathological Changes to the Kidney and Liver

Upon histopathological examination, the livers and kidneys from the non-inoculated control goslings appeared histologically normal (Figure 2A–B). However, necrosis and inflammatory cell infiltration were observed in livers of the inoculated gosling (Figure 2C). The kidneys also showed degeneration and necrosis of renal epithelial cells and inflammatory cell infiltration (Figure 2D).

Virus Load in Different Tissues

The same weight of organ samples (0.3 g) from infected goslings and controls were used to detect viral RNA using quantitative real-time PCR (qPCR) based on the ORF2 sequence, as shown in Figure 3. No goose astrovirus was detected in the control samples, whereas the virus was found in the all detected tissues of the infected birds, including the heart, liver, spleen, lung, kidney, intestine, pancreas, and brain. Among these tissues, the virus levels in the kidney and liver were higher than in the other tissues.

Changes in Serum Uric Acid, Creatinine, Calcium, and Phosphorus Levels

The serum levels of uric acid, creatinine, calcium, and phosphorus were measured using commercial kits (Figure 4). The serum level of uric acid in the inoculated goslings was significantly higher than that in the controls ($P < 0.01$) at 14 dpi, whereas there was no significant difference at 7 dpi ($P > 0.05$). However, there were no statistically significant differences in the levels of creatinine, calcium, and phosphorus between the inoculated and control goslings at 7 and 14 dpi ($P > 0.05$).

Change in XOD, ADA, PRPPAT, and PRPS1 in the Liver

The XOD and ADA activities in the liver were measured using commercial kits. As shown in Figure 5A, the XOD and ADA activities were significantly higher in the infected birds than in the controls at 7 and 14 dpi ($P < 0.05$). To further confirm this result, the mRNA levels of the 2 genes were detected using qPCR (Figure 5B). The mRNA levels of both genes were significantly increased at 7 and 14 dpi compared with those in the controls ($P < 0.05$). Phosphoribosyl pyrophosphate amidotransferase and PRPS1 are 2 import enzymes involved in purine metabolism, which are located upstream of XOD in the purine metabolism pathway. The mRNA levels of PRPPAT and PRPS1 were measured (Figure 5C). The PRPPAT mRNA level at 7 dpi and the PRPS1 mRNA level at 7 and 14 dpi were significantly higher than those in the controls ($P < 0.05$), whereas there was no statistically significant

Table 1. Primers used in this study for real-time PCR.

Primers	Accession number	Nucleotide sequence (5'-3')	Expected PCR productions size
XOD-F	NM_205127.1	GGGGAAGATGGTGAGATGGA	81 bp
XOD-R		ACGATGCGATTTGATGGGAC	
ADA-F	XM_013188525.1	CTGTCGCTTACCGAGTTTC	120 bp
ADA-R		GACGCCTTCCTTCGCTTT	
PRPPAT-F	XM_013172796.1	CAAACGCTGGATGTGGTA	174 bp
PRPPAT-R		AGACTCTGGAACGGTGCT	
PRPS1-F	XM_013183800.1	GAGCCTGCTGTGCTGAAAT	121 bp
PRPS1-R		TTGTGAATGAGGGCGAAGT	
MRP4-F	XM_013195781.1	GTGGTTCGCTGTGCGTCTG	261 bp
MRP4-R		GGTGGTGGGTGCTTGTG	

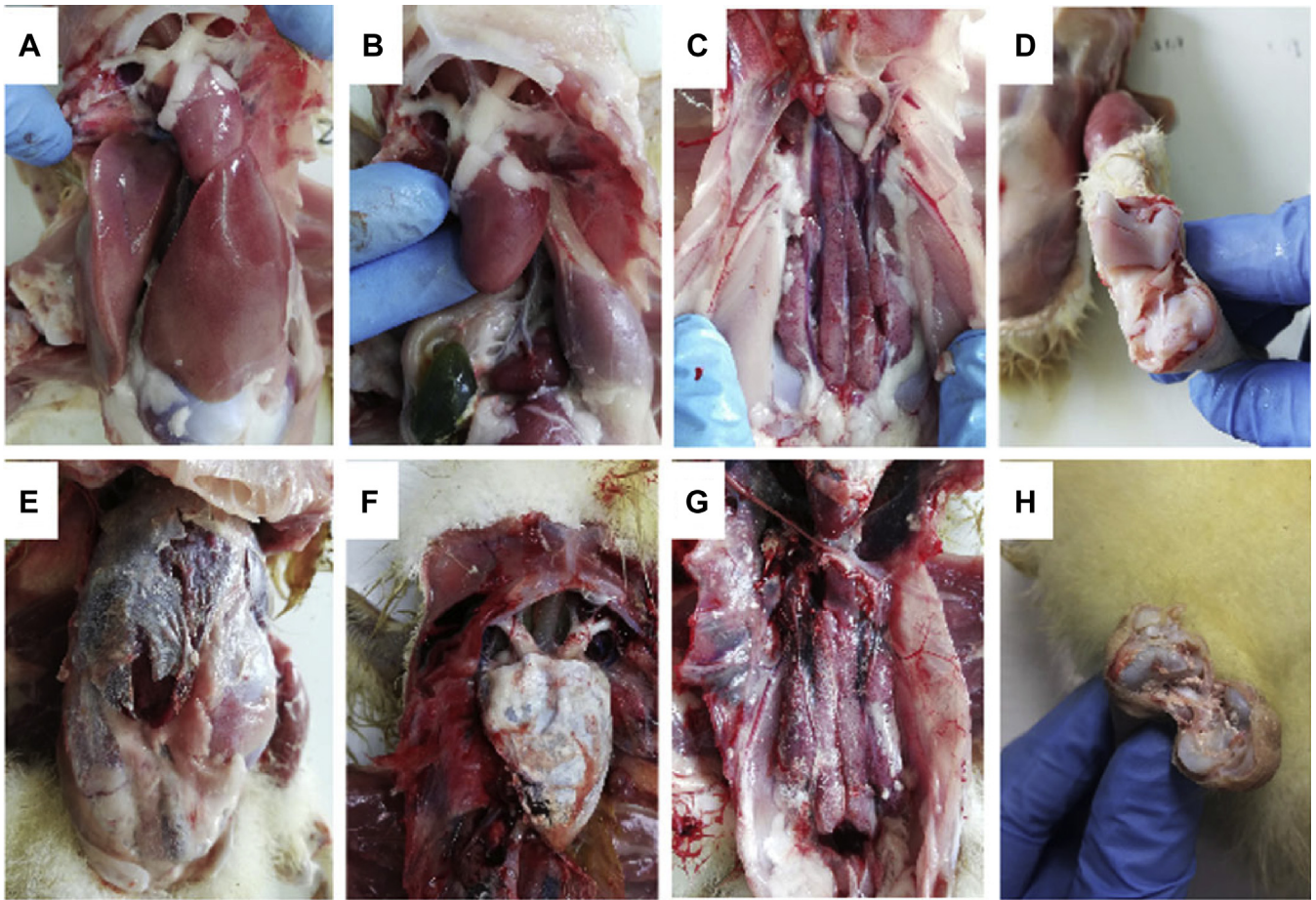


Figure 1. Gross lesions of dead goslings after inoculation with GAsV JSHA. No changes were observed in the controls (A–D), whereas dead inoculated gosling displayed uric acid deposition on the surface of the heart, liver, kidney, and articular cavity (E–H).

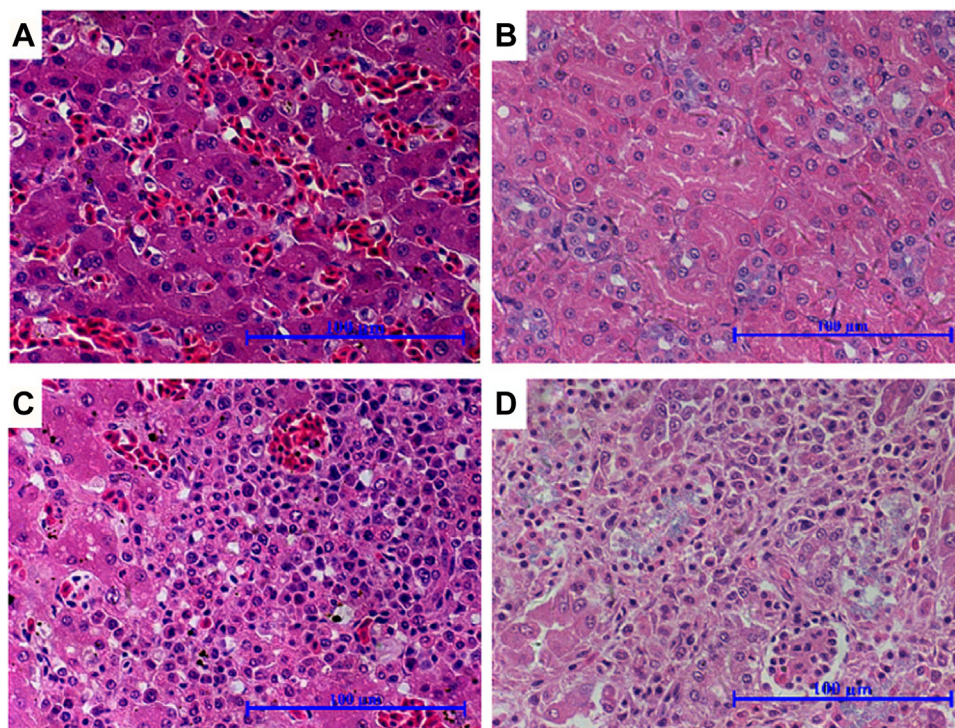


Figure 2. Histopathological changes in goslings experimentally infected with GAsV JSHA strain. All tissues from the control goslings appeared histologically normal (A–B). However, the inoculated gosling showed degeneration and necrosis of renal epithelial cells, deposition of uric acid, and inflammatory cell infiltration (C); and necrosis and inflammatory infiltration in liver (D).

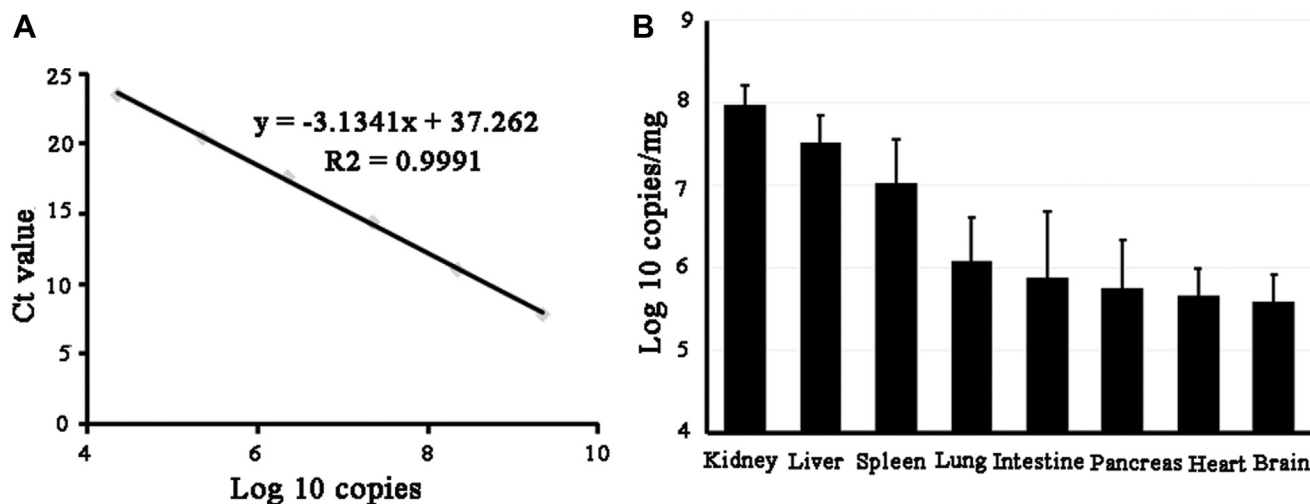


Figure 3. Virus load in organs in goslings experimentally infected with GAstV JSHA strain at 14 dpi. A 10-fold serial dilution of a known concentration of GAstV ORF2 plasmid was measured using qPCR, and the standard curve and regression equation were established. The x-axis shows the GAstV ORF2 plasmid copy number as a log 10 value, and the y-axis indicates the corresponding cycle threshold (Ct) value (A). The viral load in different organs was measured using qPCR (B). GAstV, goose astrovirus; ORF, open reading frame.

difference for the *PRPPAT* mRNA level at 14 dpi compared with that of the control ($P > 0.05$).

Change in *MRP4* Expression and Na-K-ATPase Activity in the Kidney

The *MRP4* mRNA level was measured using qPCR. As shown in Figure 6A, the mRNA levels of *MRP4* at 7 and 14 dpi were significantly lower than those of the controls ($P < 0.05$). The Na-K-ATPase activity was determined using a commercial kit. As shown in

Figure 6B, the Na-K-ATPase activities at 7 and 14 dpi were also significantly lower than those of the control ($P < 0.05$).

DISCUSSION

In the present study, 20 two-day-old goslings were injected intramuscularly with GAstV. About 25% of the infected goslings died, and typical gout pathological changes were found in the dead infected goslings, which were similar to the clinic

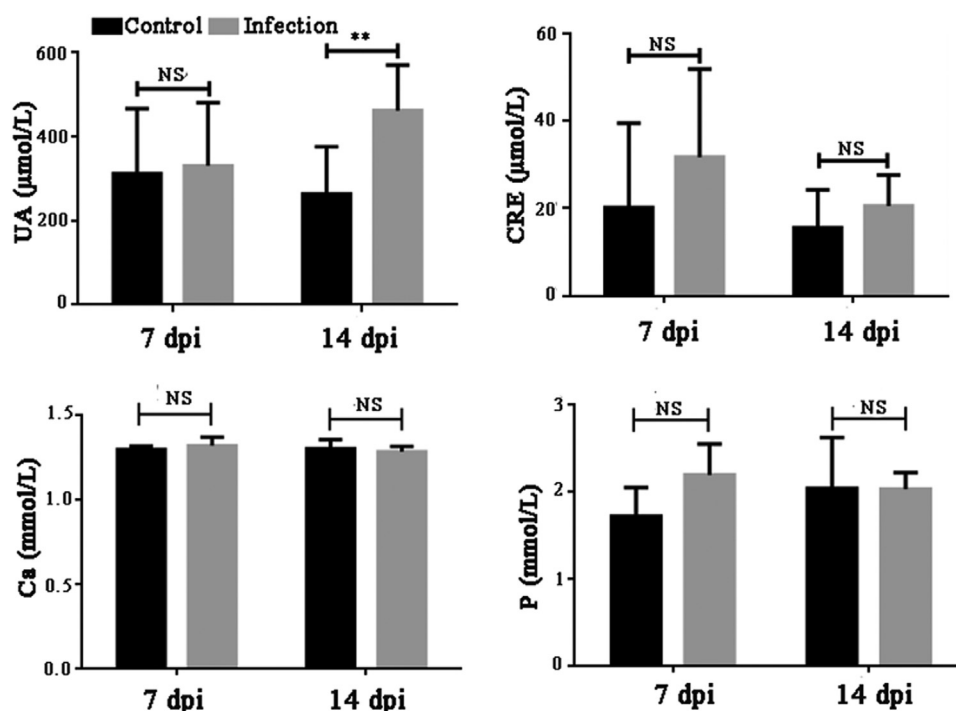


Figure 4. Changes in serum uric acid, creatinine, calcium, and phosphorus in goslings at 7 and 14 dpi after inoculation with GAstV JSHA. Value are expressed as mean \pm SD, $n = 10$. ** $P < 0.01$.

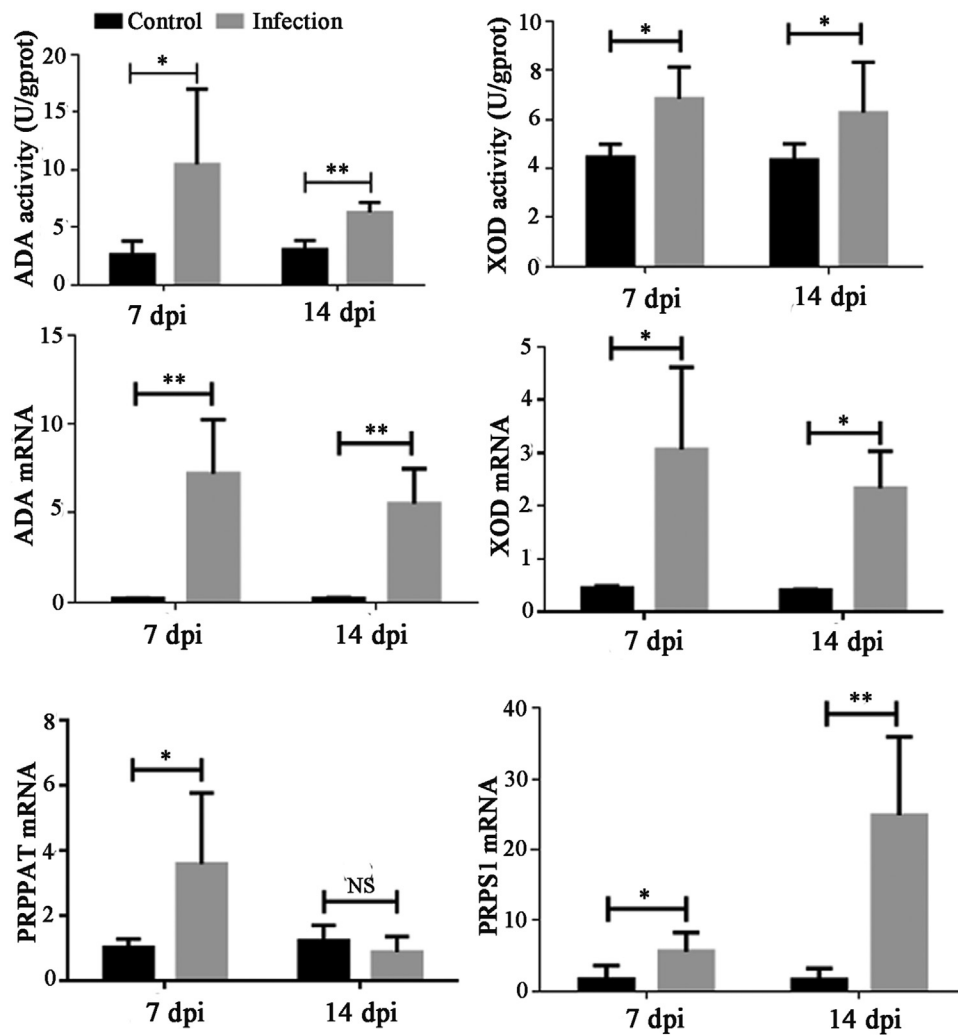


Figure 5. Changes in XOD and ADA activities, and the mRNA levels of *XOD*, *ADA*, *PRPPAT*, and *PRPS1* in the liver at 7 and 14 dpi after inoculation with GAsV JSHA. Value are expressed as mean \pm SD, n = 10. * $P < 0.05$; ** $P < 0.01$. XOD, xanthine dehydrogenase; ADA, adenosine deaminase.

symptoms of gout and the results of previous studies (Zhang et al., 2018a, 2018b; Niu et al., 2018), indicating that the gosling gout model was successfully established.

Urate is the major nitrogenous waste in birds, and gout is caused by monosodium urate crystals in presence of hyperuricemia. Our results showed that serum uric acid levels increased obviously after the goslings were

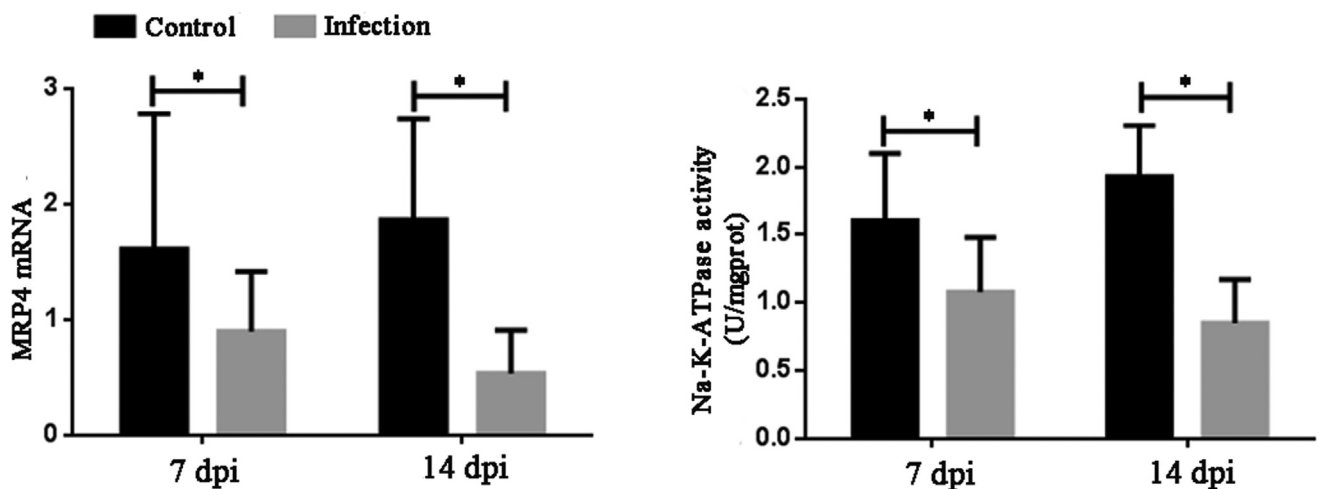


Figure 6. Changes in *MRP4* mRNA and Na-K-ATPase activities in kidney at 7 and 14 dpi after inoculation with GAsV JSHA. Value are expressed as mean \pm SD, n = 10. * $P < 0.05$. *MRP4*, multidrug resistance-associated protein 4.

infected with GAsV, indicating that virus infection might cause damages to the liver that induces purine metabolism dysfunction. This hypothesis was consistent with the determined virus load, and the histopathological changes observed in the different tissue examined. The livers of the infected goslings had the second highest virus load of all the examined organs and displayed obvious necrosis. Uric acid is the final metabolite of purine metabolism, which involves many enzymes. Xanthine dehydrogenase, which is highly expressed in the liver, is responsible for the synthesis of uric acid and oxidizes xanthine and hypoxanthine into uric acid; ADA, PRPPAT, and PRPS1 can promote the production of xanthine and hypoxanthine (Borges et al., 2002; Maiuolo et al., 2016). In the present study, the XOD and ADA activities and the mRNA levels of *XOD*, *ADA*, *PRPPAT*, and *PRPS1* increased significantly in the GAsV-infected gosling compared with those in the controls. These results demonstrated that GAsV infection promotes purine metabolism by enhancing the activities of enzymes associated with uric acid production. Similarly, nephropathogenic infectious bronchitis virus could infect chickens to cause visceral gout and increased renal xanthine oxidase mRNA transcription in broilers (Lin et al., 2015).

Hyperuricemia is not only associated with the production of uric acid but also related to excretion from the kidneys. It is reported that reduced excretion of urate is the predominant cause of hyperuricemia in human gout (Maiuolo et al., 2016). Creatinine is mainly filtered through the renal glomerulus; thus, the concentrations of creatinine in the plasma could reflect the glomerular filtration function. In the present study, no change was found in the serum level of creatinine after infection with GAsV at 7 and 14 dpi, demonstrating that GAsV infection might not damage the renal glomerulus. This was consistent with the observed in histopathological changes of the kidney; no lesions were found in the renal glomerulus, whereas renal tubules lesions were observed after GAsV infection. Degeneration and necrosis of renal epithelial cells and inflammatory cell infiltration were observed in the kidneys. In addition, kidney had the highest virus load in all the examined organs after GAsV infection. Secretion and reabsorption coexist along the length of the proximal renal tubule, and urate transporter 1 is believed to be the main contributor to urate reabsorption in humans; however, no similar sequence is present in the avian system (Bataille et al., 2011; Dalbeth, 2016). Currently, it is believed that MRP4 and OAT proteins are 2 important uric acid transport-related proteins in avians. Multidrug resistance-associated protein 4, which is located in the apical membrane of the renal proximal tubule epithelium, is believed to be the main apical membrane exit pathway for uric acid from cells to the lumen (Dudas et al., 2005; Bataille et al., 2008). Organic anion transporter 1 and OAT3 are responsible for urate transport across the basolateral membrane, relying on the generation of a sodium gradient by Na-K-ATPase

(Dudas et al., 2005; Hediger et al., 2005). In the present study, both the mRNA level of *MRP4* and the Na-K-ATPase activity were significantly lower in the infected goslings compared with those in the control, indicating that GAsV infection decreased the secretory function of the kidneys. Unfortunately, no OAT mRNA sequences have been reported in geese; therefore, the changes in OAT expression or activity after GAsV infection remain to be investigated.

In conclusion, a GAsV infection-induced gosling gout model was successfully established; GAsV infection resulted in increased XOD and ADA activities in the liver and decreased MRP4 and Na-K-ATPase activities in the kidneys, which might contribute to hyperuricemia and gout formation.

ACKNOWLEDGMENTS

This study was supported by the Priority Academic Program Development of Jiangsu Higher Education Institutions.

Conflict of Interest: The authors declare that there are no conflicts of interest.

REFERENCES

- Bataille, A. M., J. Goldmeyer, and J. L. Renfro. 2008. Avian renal proximal tubule epithelium urate secretion is mediated by MRP4. *Am. J. Physiol. Regul. Integr. Comp. Physiol.* 295:2024–2033.
- Bataille, A. M., C. L. Maffeo, and J. L. Renfro. 2011. Avian renal proximal tubule urate secretion is inhibited by cellular stress-induced AMP-activated protein kinase. *Am. J. Physiol. Ren. Physiol.* 300:1327–1328.
- Borges, F., E. Fernandes, and F. Roleira. 2002. Progress towards the discovery of xanthine oxidase inhibitors. *Curr. Med. Chem.* 9:195–217.
- Brokl, O. H., E. J. Braun, and W. H. Dantzer. 1994. Transport of PAH, urate, TEA, and fluid by isolated perfused and nonperfused avian renal proximal tubules. *Am. J. Physiol.* 266:1085–1094.
- Cortez, V., V. A. Meliopoulos, E. A. Karlsson, V. Hargest, C. Johnson, and S. Schultz-Cherry. 2017. Astrovirus biology and pathogenesis. *Annu. Rev. Virol.* 4:327–348.
- Dalbeth, N., T. R. Merriman, and L. K. Stamp. 2016. Gout. *Lancet* 388:2039–2052.
- Dudas, P. L., R. M. Pelis, E. J. Braun, and J. L. Renfro. 2005. Transepithelial urate transport by avian renal proximal tubule epithelium in primary culture. *J. Exp. Biol.* 208:4305–4315.
- Gutman, A. B., and T. F. Yü. 1972. Renal mechanisms for regulation of uric acid excretion, with special reference to normal and gouty man. *Semin. Arthritis Rheum.* 2:1–46.
- Hasegawa, M., H. Kusuhara, M. Adachi, J. D. Schuetz, K. Takeuchi, and Y. Sugiyama. 2007. Multidrug resistance-associated protein 4 is involved in the urinary excretion of hydrochlorothiazide and furosemide. *J. Am. Soc. Nephrol.* 18:37–45.
- Hediger, M. A., R. J. Johnson, H. Miyazaki, and H. Endou. 2005. Molecular physiology of urate transport. *Physiology* 20:125–133.
- Jin, M. L., X. Y. Wang, K. Ning, N. Liu, and D. B. Zhang. 2018. Genetic characterization of a new astrovirus in goslings suffering from gout. *Arch. Virol.* 163:2865–2869.
- Lin, H., Q. Huang, X. Guo, P. Liu, W. Liu, Y. Zou, S. Zhu, G. Deng, J. Kuang, C. Zhang, H. Cao, and G. Hu. 2015. Elevated level of renal xanthine oxidase mRNA transcription after nephropathogenic infectious bronchitis virus infection in growing layers. *J. Vet. Sci.* 16:423–429.

- Maiuro, J., F. Oppedisano, S. Gratteri, C. Muscoli, and V. Mollace. 2016. Regulation of uric acid metabolism and excretion. *Int. J. Cardiol.* 213:8–14.
- Mandal, A. K., and D. B. Mount. 2015. The molecular physiology of uric acid homeostasis. *Annu. Rev. Physiol.* 77:323–345.
- Nigam, S. K., and V. Bhatnagar. 2018. The systems biology of uric acid transporters: the role of remote sensing and signaling. *Curr. Opin. Nephrol. Hypertens.* 27:305–313.
- Niu, X. Y., J. J. Tian, J. Yang, X. N. Jiang, H. Z. Wang, H. Chen, Y. Tang, and Y. X. Diao. 2018. Novel goose astrovirus associated gout in gosling, China. *Vet. Microbiol.* 220:53–56.
- Sandhu, T. S., B. W. Calnek, and L. Zeman. 1992. Pathology and serologic characterization of a variant of duck hepatitis type I virus. *Avian Dis.* 36:932–936.
- Smyth, V. J. 2017. A Review of the strain Diversity and pathogenesis of chicken astrovirus. *Viruses* 9:29.
- Todd, D., V. J. Smyth, N. W. Ball, B. M. Donnelly, M. Wylie, N. J. Knowles, and B. M. Adair. 2009. Identification of chicken enterovirus-like viruses, duck hepatitis virus type 2 and duck hepatitis virus type 3 as astroviruses. *Avian Pathol.* 38:21–30.
- Yang, J., J. J. Tian, Y. Tang, and Y. X. Diao. 2018. Isolation and genomic characterization of gosling gout caused by a novel goose astrovirus. *Transbound. Emerg. Dis.* 65:1689–1696.
- Yuan, X., K. Meng, Y. Zhang, Z. Yu, W. Ai, and Y. Wang. 2019. Genome analysis of newly emerging goose-origin nephrotic astrovirus in China reveals it belongs to a novel genetically distinct astrovirus. *Infect. Genet. Evol.* 67:1–6.
- Zhang, Q. S., Y. X. Cao, J. Wang, G. H. Fu, M. X. Sun, L. J. Zhang, L. Meng, G. L. Cui, Y. Huang, X. Y. Hu, and J. L. Su. 2018a. Isolation and characterization of an astrovirus causing fatal visceral gout in domestic goslings. *Emerg. Microbes Infect.* 7:71.
- Zhang, X. Y., D. Ren, T. F. Li, H. Y. Zhou, X. Y. Liu, X. B. Wang, H. Lu, W. Gao, Y. J. Wang, X. Y. Zou, H. C. Sun, and J. Q. Ye. 2018b. An emerging novel goose astrovirus associated with gosling gout disease. *China. Emerg. Microbes Infect.* 7:152.